

A Wedge Diffraction Based Scattering Model for Acoustic Scattering from Rough Littoral Seafloors

Richard S. Keiffer
Robert A. Zingarelli
Naval Research Laboratory
Stennis Space Center, MS 39529 USA

Abstract - Models for acoustic scattering from rough surfaces based on Biot and Tolstoy's (BT) exact wedge diffraction theory have proven accurate and useful in a number of experimental and numerical studies [1]. Because the BT solution is restricted to impenetrable wedges (acoustically hard or soft boundary conditions), scattering models based on the BT solution have thus far been limited to the rough air/sea interface where the actual boundary conditions are very nearly pressure-release (soft). Recently, important theoretical work [2,3] has extended the exact BT theory to density-contrast but isospeed wedges. This new development makes possible the application of wedge diffraction based scattering models to the roughness at the sea floor where the change in the acoustic impedance at the boundary is dominated by changes in density and only weakly affected by changes in sound speed. However, it is important to confirm that small amounts of sound speed contrast do not perturb the diffraction too much. To contribute to the understanding of how the diffracted wave is affected by sound speed contrast and get some idea as to the practical limitations of wedge-diffraction based scattering models for littoral seafloors, a simple numerical experiment involving a highly accurate Finite-Difference Time-Domain (FDTD) solution to the acoustic wave equation and a wedge-shaped boundary has been explored. This paper presents the results of FDTD experiments designed to quantify any changes in the diffracted field brought about by sound speed contrast. An ad hoc treatment of sound speed contrast is developed based on the requirement that the diffracted wave must smooth out the reflection discontinuity and preserve the continuity of the total field.

I. INTRODUCTION

Models for acoustic scattering from rough surfaces based on Biot and Tolstoy's (BT) exact wedge diffraction theory [1] have proven accurate and useful in a number of experimental and numerical studies [2-7]. Of particular importance to the ocean-acoustic modeling community, which deals with surfaces having significant roughness across a large range of scales, is this modeling approaches ability to efficiently compute the impulse response directly in the time domain. For a rough 2D surface, discretely sampled and measuring M points on a side, the calculation of a single-scatter approximation to the impulse response is proportional to M^2 . This kind of efficiency has allowed a model based on BT wedge diffraction theory to be used in very demanding simulations, for example, in large Monte Carlo calculations for the average Doppler spectrum of acoustic signals backscattered from time-evolving, two-dimensional sea surfaces [7].

Because the BT solution is restricted to impenetrable wedges (acoustically hard or soft boundary conditions), scattering models based on the BT solution have thus far been limited to the rough air/sea interface where the actual boundary conditions are very nearly pressure-release (soft). Recently, important theoretical work [8,9] has extended the exact BT theory to density-contrast but isospeed (diaphanous) wedges. This new development makes possible the application of wedge diffraction based scattering models to the roughness at the sea floor. In particular, rough littoral sediments appear to be good candidates for the application of such models. As Table I makes clear, for these seafloors the change in the acoustic impedance at the boundary is dominated by changes in density and only weakly affected by changes in sound speed.

Sediment Type	Sediment / Water Sound Speed Ratio	Sediment / Water Density Ratio
Coarse Sand	1.20	2.03
Fine Sand	1.15	1.96
Sandy Silt	1.10	1.77
Clay	0.98	1.35

Table 1. Types of seafloor sediments typical of littoral regions and their sound speeds (25 kHz) and densities relative to the overlying ocean water. Data taken from Ref. [10].

Although the potential utility of a density-contrast model for the seafloor is certainly supported by the geoaoustic parameters listed in Table I, it is important to confirm that small amounts of sound speed contrast do not perturb the diffraction too much. There are reasons to be cautious. So far as it is known at this time, the mathematics of wedge diffraction problem becomes much more difficult when change in the sound speed (even small perturbations) are contemplated. This could mean that the scattering physics itself is quite sensitive to changes in the sound speed contrast. It is clear that the controlling physics in this transition

Report Documentation Page

Form Approved
OMB No. 0704-0188

Public reporting burden for the collection of information is estimated to average 1 hour per response, including the time for reviewing instructions, searching existing data sources, gathering and maintaining the data needed, and completing and reviewing the collection of information. Send comments regarding this burden estimate or any other aspect of this collection of information, including suggestions for reducing this burden, to Washington Headquarters Services, Directorate for Information Operations and Reports, 1215 Jefferson Davis Highway, Suite 1204, Arlington VA 22202-4302. Respondents should be aware that notwithstanding any other provision of law, no person shall be subject to a penalty for failing to comply with a collection of information if it does not display a currently valid OMB control number.

1. REPORT DATE SEP 2008	2. REPORT TYPE	3. DATES COVERED 00-00-2008 to 00-00-2008			
4. TITLE AND SUBTITLE A Wedge Diffraction Based Scattering Model for Acoustic Scattering from Rough Littoral Seafloors		5a. CONTRACT NUMBER			
		5b. GRANT NUMBER			
		5c. PROGRAM ELEMENT NUMBER			
6. AUTHOR(S)		5d. PROJECT NUMBER			
		5e. TASK NUMBER			
		5f. WORK UNIT NUMBER			
7. PERFORMING ORGANIZATION NAME(S) AND ADDRESS(ES) Naval Research Laboratory, Stennis Space Center, MS, 39529		8. PERFORMING ORGANIZATION REPORT NUMBER			
9. SPONSORING/MONITORING AGENCY NAME(S) AND ADDRESS(ES)		10. SPONSOR/MONITOR'S ACRONYM(S)			
		11. SPONSOR/MONITOR'S REPORT NUMBER(S)			
12. DISTRIBUTION/AVAILABILITY STATEMENT Approved for public release; distribution unlimited					
13. SUPPLEMENTARY NOTES See also ADM002176. Presented at the MTS/IEEE Oceans 2008 Conference and Exhibition held in Quebec City, Canada on 15-18 September 2008.					
14. ABSTRACT see report					
15. SUBJECT TERMS					
16. SECURITY CLASSIFICATION OF:			17. LIMITATION OF ABSTRACT Same as Report (SAR)	18. NUMBER OF PAGES 7	19a. NAME OF RESPONSIBLE PERSON
a. REPORT unclassified	b. ABSTRACT unclassified	c. THIS PAGE unclassified			

regime is not well understood. To contribute to the understanding of how the diffracted wave is affected by sound speed contrast and get some idea as to the practical limitations of wedge-diffraction based scattering models for littoral seafloors, a simple numerical experiment involving a highly accurate Finite-Difference Time-Domain (FDTD) solution to the acoustic wave equation and a wedge-shaped boundary has been explored. This paper presents the results of FDTD experiments designed to quantify any changes in the diffracted field brought about by sound speed contrast. These numerical experiments show that in general the impact of sound speed contrast on the diffracted wave is proportional to the overall change in characteristic acoustic impedance. However, when the scattering direction approaches a reflection boundary, the impact of sound speed contrast on the diffracted wave is significantly greater. Wedge diffraction theory provides an explanation for these results and it is shown in this paper that the angular dependence introduced by sound speed contrast can be predicted from the simple fact that in the vicinity of the reflection boundary the diffracted wave acts to smooth out the reflection discontinuity and preserve the continuity of the total field.

II. NUMERICAL EXPERIMENT AND DATA CHARACTERIZATION

The details of the FDTD model used in this study (named FIDO) have been described elsewhere [11] and are similar to other implementations found in the literature [12]. FIDO solves the two-dimensional linear acoustic wave equation in a second order accurate algorithm assuming a nondispersive, non-attenuating medium. In previous studies [13], FIDO was tested (with excellent agreement) for backscattering from impenetrable wedge shaped boundaries using exact wedge diffraction theory and other FDTD results as benchmarks.

Figure 1 shows a sketch of one of the numerical experiments. An example of the “source to wedge-apex to receiver “ path that is of primary interest in this study is indicated. Also depicted are “reflected” paths that may arrive (in time) in the vicinity of the apex-diffracted wave. Ten receivers were arranged in the fluid medium exterior to the wedge and equidistant from the wedge apex in order to observe the diffracted wave traveling into different directions.

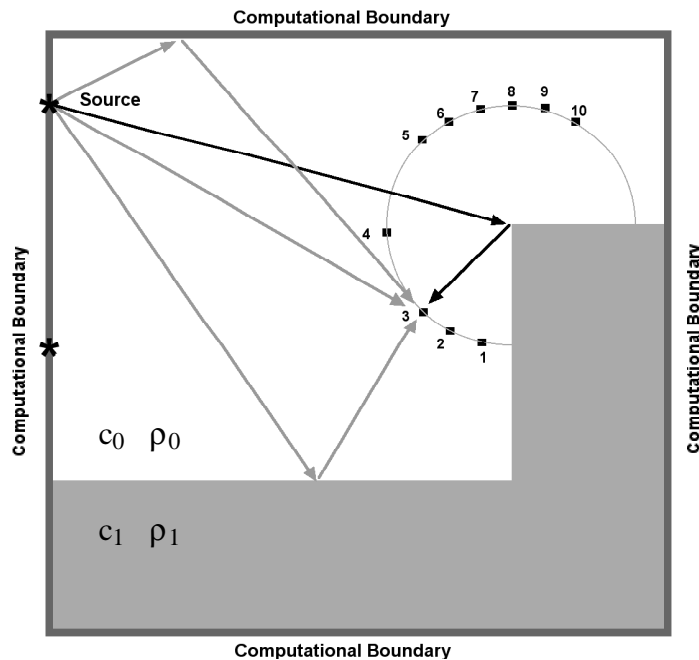


Fig. 1 Schematic of FDTD numerical experiment to isolate diffracted waves from 90° wedge and examine implications of sound speed contrast.

The density ($\rho_0 = 1.0 \text{ g/cm}^3$) and sound speed ($c_0 = 1500 \text{ m/s}$) in the fluid medium exterior to the wedge remained fixed while the density and sound speed interior to the wedge shaped boundary varied. Parameter values typical of sand ($\rho_1 = 2.03 \text{ g/cm}^3$), with the sound speed ratio varying ($1.05 < c_1/c_0 < 1.23$), typical of silt ($\rho_1 = 1.77 \text{ g/cm}^3$), with ($1.04 < c_1/c_0 < 1.08$), and typical of clay ($\rho_1 = 1.35 \text{ g/cm}^3$) with ($0.98 < c_1/c_0 < 1.04$) were considered (see Ref. [10]). The specific parameter values used in the study are listed in Table II.

Sediment Type	Sediment Sound Speeds	Sediment Density
Sand	1500, 1560, 1620, 1700, 1800	2.03
Silt	1500, 1560, 1620	1.77
Clay	1475, 1500, 1560	1.35

Table II. Typical (sand, silt and clay) sounds speeds and densities used in the numerical studies for the interior of the wedge shaped boundary.

Analysis of the FDTD experiments consisted of identifying the apex-diffracted wave and isolating it from the direct waveform that arrives before it and from any reflected paths that arrive after it. The source waveform was a Ricker wavelet (a twice differentiated Gaussian) $s(t) = -2\alpha(2\alpha t^2 - 1)e^{-\alpha t^2}$ with total duration of 0.0525 s. Using $\alpha = 1200.0$, this waveform is centered at approximately 31 Hz. The duration of the pulse, and the time separation of the diffracted wave from other arrivals limited the receiver locations to the ones used in the study. Figure 2 shows the typical data collected at receiver no. 3 for the numerical experiment depicted in Fig. 1 (a diffracted angle of 30° measured from the vertical face of the wedge). In this particular example, the wedge shaped boundary had a density appropriate for sand ($\rho_1 = 2.03 \text{ g/cm}^3$) and the sound speed ranged from 1500 m/s (the isospeed wedge) to 1800 m/s. Note that changing the sound speed interior to the wedge affects the amplitude of the diffracted wave but the shape of the diffracted waveform appears to be unchanged.

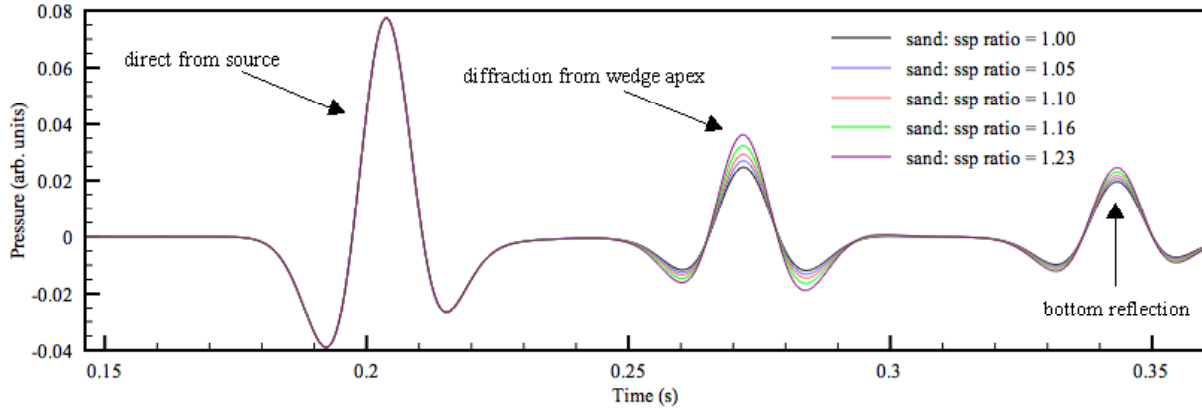


Fig. 2 Calculated pressure time series from the FDTD code FIDO at receiver location 3.

Once isolated, the peak value of the diffracted wave was recorded and normalized by the peak amplitude of the apex-diffracted wave for the isospeed case. The normalized FDTD data for the sand and clay wedges are displayed in Figs. 3 and 4. The results show that one effect that sound speed contrast has on the diffracted wave is to introduce a θ_R - dependence in its magnitude.

These plots (and other data not shown here) make clear that for all three littoral wedge types (sand, silt, clay), the impact of sound speed contrast on the diffracted wave varies with the propagation direction of the diffracted wave. Away from the reflection boundaries, say $70^\circ \leq \theta_R \leq 150^\circ$, the angle dependence is weak and the effect of sound speed contrast on the magnitude of the diffracted wave seems to scale accurately with the sound speed ratio. The FDTD results show some angular dependence in the normalized diffracted wave for all three sediment types (sand, silt, clay). For sand the effect is most clear, there is a 30 % change in the normalized amplitude of the diffracted wave over a 60° span. Somewhat less sensitive to the direction of the diffracted wave was the silt wedge (not shown) and the clay wedge showed the least angular variation. The clay wedge was unique in that it presented the only example of a normalized diffraction amplitude that decreased near the reflection boundary.

III. THE DIFFRACTED WAVE

For this acoustic problem, the apex- diffracted wave is the part of the total field not accounted for by the geometric term in the decomposition:

$$p(r, \theta, z, t) = G(r, \theta, z, t) + D(r, \theta, z, t) \quad (1)$$

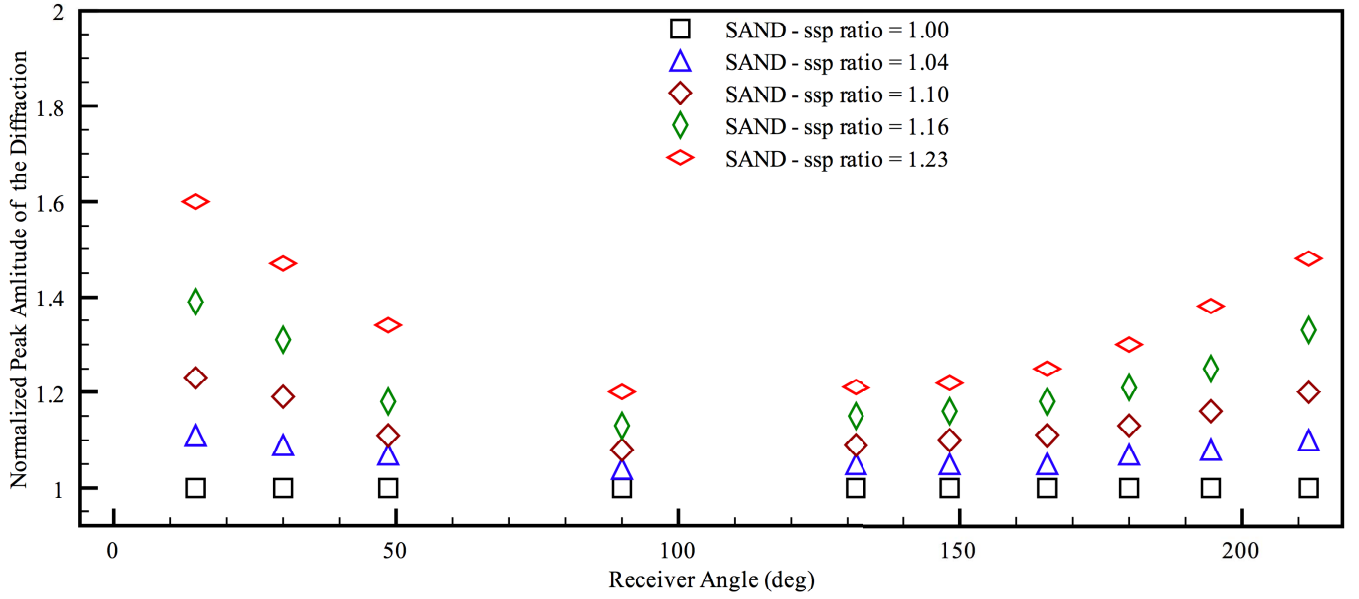


Fig. 3 Magnitude of normalized diffraction from a sand wedge shown as a function of receiver angle (deg).

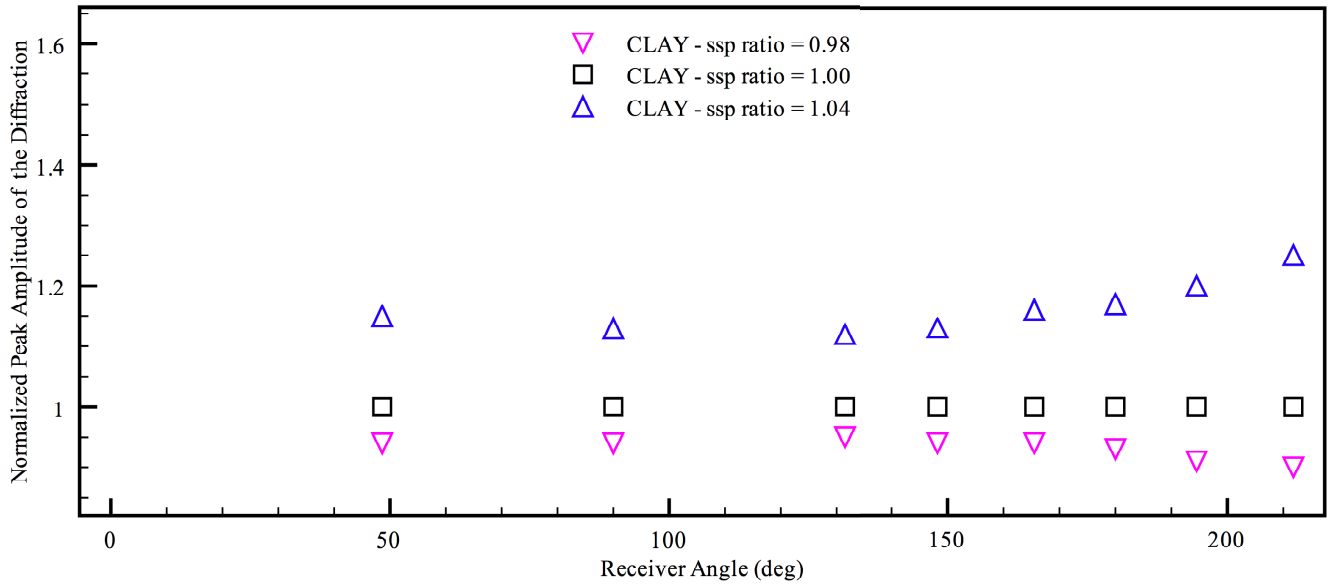


Fig. 4 Magnitude of normalized diffraction from a clay wedge shown as a function of receiver angle (deg).

The geometric term includes the direct wave from the source plus any reflections from the faces of the wedge. To our knowledge, there are two different exact solutions for the impulse response of an infinitely long, density-contrast wedge. Using Davis and Scharstein solution [9], the diffracted wave in the exterior region (the region that includes the source) is:

$$D(r, \theta, z, t) = \frac{c}{2\pi r_0 r \sin \eta} \sum_{n=1}^{\infty} S(\xi, \theta, v_n^s) \pm \frac{c}{2\pi r_0 r \sin \eta} \sum_{m=1}^{\infty} A(\xi, \theta, v_m^a) \quad (2)$$

where,

$$S(\xi, \theta, v_n^s) = \frac{e^{-v_n^s \xi} \sin(v_n^s \pi) (\cos v_n^s \pi + \Gamma \cos v_n^s (\pi - 2\alpha)) \cos v_n^s (\pi - \phi_0) \cos v_n^s (\pi - \phi)}{\pi \cos v_n^s \pi + \Gamma (\pi - 2\alpha) \cos v_n^s (\pi - 2\alpha)} \quad (3)$$

$$A(\xi, \theta, v_m^a) = \frac{e^{-v_m^a \xi} \sin(v_m^a \pi) (\cos v_m^a \pi - \Gamma \cos v_m^a (\pi - 2\alpha)) \sin v_m^a (\pi - \phi_0) \sin v_m^a (\pi - \phi)}{\pi \cos v_m^a \pi - \Gamma (\pi - 2\alpha) \cos v_m^a (\pi - 2\alpha)}$$

and $\Gamma = (\rho_1 - \rho_0) / (\rho_1 + \rho_0)$. Note that the sum indicated in Eq. 2 is over all v_n^s and v_m^a . These eigenvalues are determined by solving the transcendental equations:

$$\sin v\pi + \Gamma \sin v(\pi - 2\alpha) = 0 \quad (4a)$$

$$\sin v\pi - \Gamma \sin v(\pi - 2\alpha) = 0 \quad (4b)$$

IV. MODELING DIFFRACTION FROM SOUND SPEED AND DENSITY CONTRAST WEDGES

In Ref. [9], Davis and Scharstein point out that “the diffracted wave is most important in the vicinity of geometric (ray) boundaries, where its primary role is to smooth out the step discontinuities in the geometric acoustic field”. At the reflection boundary, for example, this discontinuity is proportional to Γ and at the shadow boundary (which there are non in this experiment) the discontinuity is proportional to Γ^2 . Now, it is important to note that this aspect of the diffracted wave is a consequence of the step-discontinuity in the geometric component not of the material properties of the wedge. Therefore, the observation of Davis and Scharstein should hold when there is both density and sound speed contrast are part of the wedge problem. In this case though, the diffracted field in the vicinity of a reflection boundary should be approximately proportional the plane wave reflection coefficient:

$$\Gamma_{eff} = \frac{\rho_1}{\rho_0} - \frac{c_1}{c_0} \cos \theta_1 \quad \frac{\rho_1}{\rho_0} + \frac{c_1}{c_0} \cos \theta_1^{-1}, \quad (5)$$

where $\cos \theta_1 = c_1 \cos \theta_0 / c_0$. This suggests that for receivers in the vicinity of the reflection boundary it may be possible to trick the density-contrast solution into mimicking the effects of sound speed contrast. To do this first use the reflection coefficient shown above to compute modified eigenvalues v_n^s and v_m^a from Eqs. 4 and then use these modified eigenvalues in Eq. 2 to compute the diffraction. There are of course two reflection boundaries in this experiment and a receiver may be in the vicinity of one or the other or neither. When the receiver is not in the vicinity of either reflection boundary, it can be ambiguous which wedge face, that is which angle of incidence, to use. For this experiment, an algorithm was developed that allows for smooth transitions from one reflection boundary to the other: If the source and receiver are on the same side of the wedge bisector then measure angles relative to the vertical wedge face or its imaginary extension. Fig 5 illustrates this case and shows a progression of receivers all of which have associated with them reflection coefficients calculated relative to the horizontal wedge face.

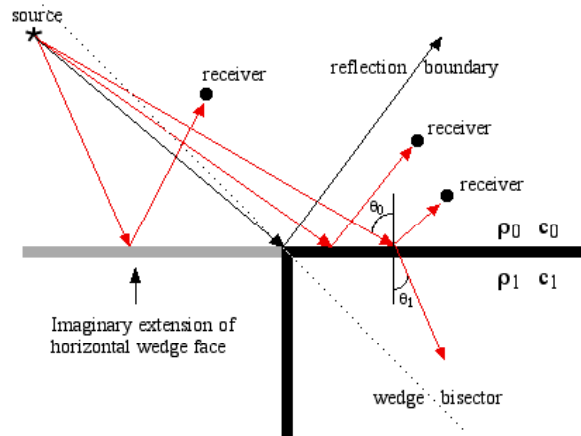


Fig. 5 Schematic drawing illustrating geometry of reflection coefficient calculation for source and receivers on opposite side of wedge bisector.

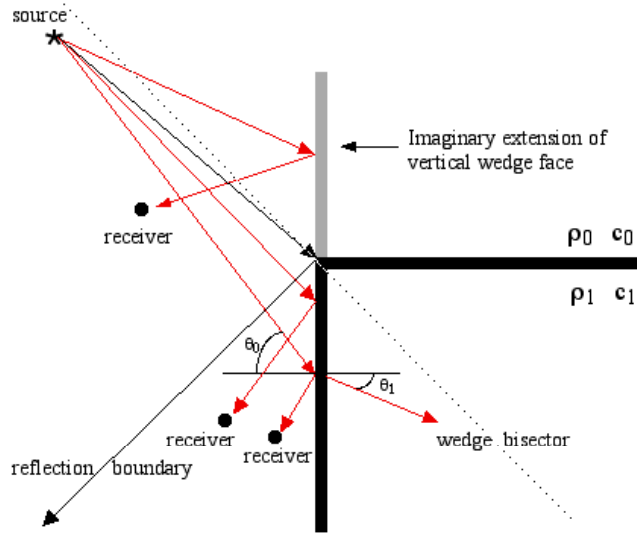


Fig. 6 Schematic drawing illustrating geometry of reflection coefficient calculation for source and receivers on opposite side of wedge bisector.

V. MODEL COMPARISONS

To test this ad hoc extension, the exact density contrast wedge diffraction solution (Eqs. 2 and 4) was computed for different sound speed ratios using the plane wave reflection coefficient for a sound speed and density contrast plane (Eq. 5) and the algorithm describe above. Again the isospeed density contrast wedge diffraction amplitude was used to normalize the results. Shown in Fig. 6 and Fig. 7 are the new model results overlying the FDTD results shown earlier. It can be seen that this simply ad hoc treatment does a really good job of replicating the effect that sound speed contrast has on the diffracted field over all propagation directions. This is true for the sand wedge where the impact of sound speed contrast resulted in a significant dependence on propagation direction and it is true for the clay wedge which showed a weak angular dependence. Importantly for the clay wedge, the ad hoc model captures the declining normalized diffraction magnitude near the reflection boundary when the sound speed in the wedge was slower than in the overlying fluid medium.

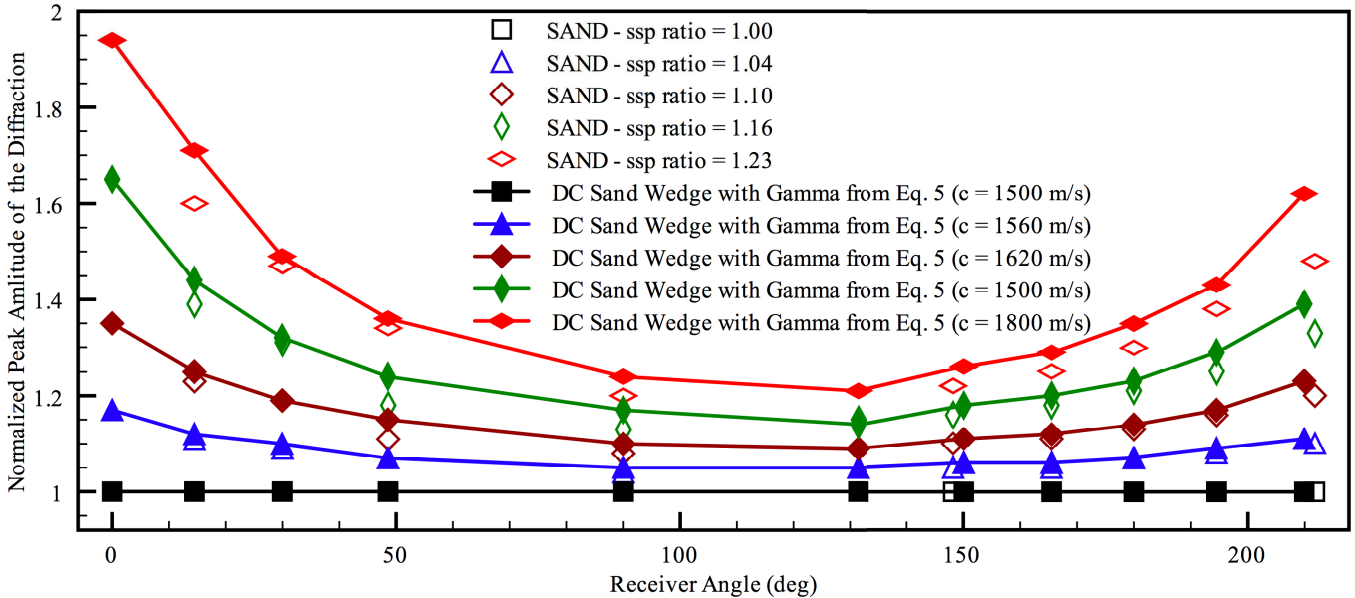


Fig. 7 FDTD results for the sand wedge and modeled results that used the exact density-contrast solution modified by an ad hoc reflection coefficient

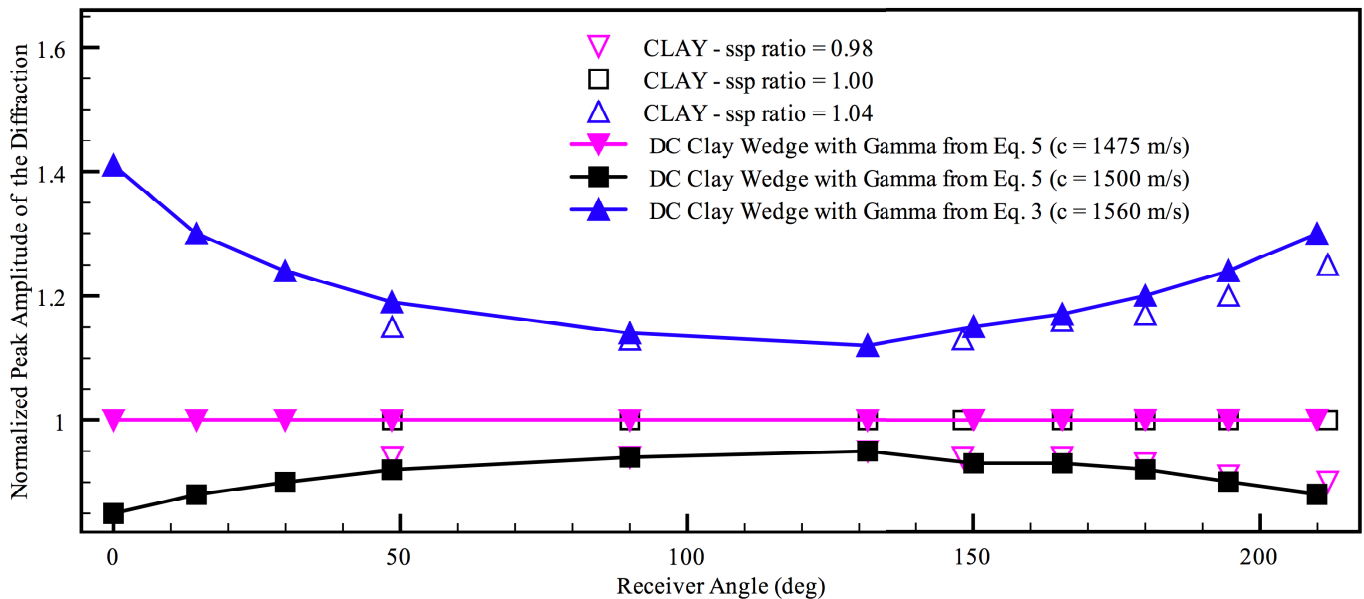


Fig. 8 FDTD results for the clay wedge and modeled results that used the exact density-contrast solution modified by an ad hoc reflection coefficient

There are two main conclusions that can be drawn from these results. First, acoustic scattering from many rough littoral sediments can be modeled accurately with a density-contrast only approximation for the boundary condition. This approximation seems to generally hold better for sediments composed of silts and clays than sand but even for sand it works well if the receiver is away from the specular direction (reflection boundary). Second, the density-contrast wedge diffraction solution can be manipulated using an ad hoc reflection coefficient so that it can predict the diffraction from wedges that have sound speed and density contrast. These results suggest that already proven models like the wedge assemblage method [2-7], an approach based on wedge diffraction but previously limited to pressure-release, hard, or density contrast boundaries, can accurately be applied to many rough littoral seafloors.

ACKNOWLEDGEMENT

The authors recognize and is thankful for numerous useful technical discussions with Drs. C. Feuillade and D. Lindwall. This document, NRL/MM/7180-08-083, has been reviewed and is approved for public release.

REFERENCES

- [1] M. A. Biot and I. Tolstoy, "Formulation of Wave Propagation in Infinite Media by Normal Coordinates with Application to Diffraction," *J. Acoust. Soc. Am.*, 29, 381-391, (1957).
- [2] H. Medwin, "Shadowing by a Finite Noise Barrier," *J. Acoust. Soc. Am.*, 69, 1060-1064 (1981).
- [3] W. A. Kinney, C. S. Clay, and G. A. Sandness, "Scattering from a Corrugated Surface: Comparison Between Experiment, Helmholtz-Kirchhoff Theory, and the Facet-Ensemble Method," *J. Acoust. Soc. Am.*, 73, 183-194 (1983).
- [4] R. S. Keiffer, "On the Validity of the Wedge Assemblage Method for Pressure-Release Sinusoids," *J. Acoust. Soc. Am.*, 93, 3158-3168 (1993).
- [5] R. S. Keiffer, J. C. Novarini, and G. V. Norton, "The Impulse Response of an Aperture: Numerical Calculations within the Framework of the Wedge Assemblage Method," *J. Acoust. Soc. Am.*, 95, 3-12 (1994).
- [6] R. S. Keiffer and J. C. Novarini, "A Time Domain Rough Surface Scattering Model Based on Wedge Diffraction: Application to Low-Frequency Backscattering from Two-Dimensional Sea Surfaces," *J. Acoust. Soc. Am.*, 107, 27-39 (2000).
- [7] R. S. Keiffer, J. C. Novarini, and R.W. Scharstein, "A Time-Variant Impulse Response Method for Acoustic Scattering from Moving Two-Dimensional Surfaces," *J. Acoust. Soc. Am.*, 118, 1283- 1299 (2005).
- [8] D. Chu, "Exact Solution for a Density-Contrast Shallow Water Wedge using Normal Coordinates," *J. Acoust. Soc. Am.*, 87, 2442-2450 (1990).
- [9] A. M. J. Davis and R. W. Scharstein, "The Complete Extension of the Biot-Tolstoy Solution to the Density-Contrast Wedge with Sample Calculations," *J. Acoust. Soc. Am.*, 101, 1821-1835 (1997).
- [10] E. L. Hamilton, "Geoacoustic Modeling of the Sea Floor," *J. Acoust. Soc. Am.*, 68, 1313-1340, (1980).
- [11] R. A. Zingarelli, "Finite Difference Solutions to the Workshop Problems," in *Proceedings of the Reverberation and Scattering Workshop*, edited by D. B. King, S. A. Chin-Bing, J. A. Davis, and R. B. Evans, May 1994, Gulfport, MS, 3.148-3.166, Naval Research Laboratory Book Contribution NRL/BE/7181-96-001.
- [12] R. M. Alford, K. R. Kelly, and D. M. Boore, "Accuracy of finite-difference modeling of the acoustic wave equation," *Geophysics* 39, 834-842 (1974).
- [13] R. S. Keiffer, J. C. Novarini, and R. A. Zingarelli, "Finite-Difference Time-Domain Modeling of Low to Moderate Frequency Sea Surface Reverberation in the Presence of a Near-Surface Bubble Layer," *J. Acoust. Soc. Am.*, 110, 782-785 (2001).